PROCEEDINGS OF SCIENCE

TMD densities from the Parton branching method

Radek Žlebčík*
DESY
E-mail: radek.zlebcik@desy.de

We present results from a Parton branching solution of the DGLAP equation at LO, NLO and NNLO which is is capable to extract both the collinear part and the transverse momentum dependent part of the parton densities. We demonstrate that within our method the collinear part of parton densities exactly corresponds to the semi-analytical solution of the DGLAP equation up to NNLO. Moreover, we study the transverse momentum of parton densities with respect to the parton flavour, ordering condition used during the evolution and the intrinsic momentum.

XXV International Workshop on Deep-Inelastic Scattering and Related Subjects
3-7 April 2017
University of Birmingham, UK

*Speaker.

PoS(DIS2017)078

1. Introduction

We discus some aspects of the Parton branching evolution method recently developed in [1, 2]. This formalism can be compared with existing evolution equations working in the special part of the phase space: CSS at low transverse momentum [3] and/or CCFM at high energy and low-x region [4]. Our approach is rather general and we believe it can be further improved i.e. by transverse splitting functions [5].

2. Method description

In our approach, we are using the evolution equation which deals separately with the resolvable and non-resolvable branchings. Introducing the resolution parameter z_m the emissions with $z < z_m$ are considered as resolvable whereas the emissions with $z > z_m$ are resummed together with the virtual terms. The variable z is the fraction of the light-cone momentum of the parton after the branching with respect to the original one. The non-resolvable emissions and the virtual terms are resummed using the Sudakov form factor which leads to the following evolution equation in scale μ^2 for the momentum weighted PDFs $\tilde{f}_a(x,\mu^2) = x f_a(x,\mu^2)$:

$$\frac{\mathrm{d}}{\mathrm{d}\ln\mu^2}\frac{\tilde{f}_a(x,\mu^2)}{\Delta_a(\mu^2)} = \sum_b \int_x^{z_m} \frac{\mathrm{d}z}{z} z P_{ab}(\mu^2,z) \frac{\tilde{f}_b(x/z,\mu^2)}{\Delta_a(\mu^2)}, \tag{2.1}$$

where the Sudakov form factor $\Delta_a(\mu^2)$ is defined as:

$$\Delta_a(\mu^2) = \exp\left(-\int_{\mu_0^2}^{\mu^2} \frac{\mathrm{d}\mu^2}{\mu^2} \sum_b \int_0^{z_m} \mathrm{d}z z P_{ba}(\mu^2,z)\right) \tag{2.2}$$

and can be interpreted as a probability that parton a does not undergo any resolvable branching between the starting scale of the evolution μ_0^2 and μ^2. Note that in both equations (2.1), (2.2) the upper limit for integration over z is $z_m < 1$ which means that we do not include the possible virtual part of the splitting functions P_{ab} at $z = 1$. Moreover, it can be shown that such evolution equation (2.1) automatically conserves unitarity irrespectively to the particular form of the splitting functions which is a consequence of the Sudakov resummation of high-z branchings. That means that if the total momentum fraction S carried by the proton

$$S(\mu^2) = \sum_a \int_0^1 \mathrm{d}x \tilde{f}_a(x,\mu^2) \tag{2.3}$$

is at scale μ_0^2 is $S(\mu_0^2) = 1$ then this relation also holds for evolved PDFs at higher scales.

In case that P_{ab} corresponds to standard DGLAP splitting functions, it can be shown that also the evolution (2.1) converges to the DGLAP equation

$$\frac{\mathrm{d}\tilde{f}_a(x,\mu^2)}{\mathrm{d}\ln\mu^2} = \sum_b \int_x^1 \frac{\mathrm{d}z}{z} z P_{ab}(\mu^2,z) \tilde{f}_b(x/z,\mu^2), \tag{2.4}$$

if z_m is large enough. On the other hand, the automatic unitarity conservation and non-necessity to know the virtual terms of the splittings makes equation (2.1) a good candidate for possible

extensions beyond standard DGLAP. In particular, we already tested the effect of scale dependent resolution scale $z_m(\mu^2)$ on the evolution. In future, we plan to extend the splittings for the CCFM terms which are important in low-x limit.

The evolution equation (2.1) can be transformed to the integral equation of Volterra-type which is a special case of the Fredholm-type integral equation where the resulting functions for a particular value of the scale (evolution variable) depend only on the functions at lower scales. There are several possibilities how to solve such equations. Motivated by easy implementation and extensibility and good control over the uncertainties we decided for Monte Carlo technique which employs Markov chain of the branching to solve equation (2.1). Within this method the $\Delta_a(\mu_2^2)/\Delta_a(\mu_1^2)$ is employed as a non-branching probability between two consequent scales μ_1^2 and μ_2^2 and the splitting function integrated over $z < z_m$ represents the branching probability. The method is described in more detail in [2].

This procedure is graphically explained in Fig. 1 where the equation (2.1) is solved by MC method for two values of the resolution parameter z_m. It can be seen, as expected, that the number of branchings strongly depends on the z_m value, for $z_m \to 1$ the integral over z in the Sudakov factor even goes to infinity. It is nicely visible that for $z_m = 1 - 10^{-6}$ there are more soft emissions with $z \to 1$ (vertical lines) than for $z_m = 1 - 10^{-2}$. On the other hand, we tested that the obtained PDFs for these two cases are nearly identical [2].

In [1, 2] we demonstrated that at LO and NLO these PDFs from Parton branching method are within 1% identical with the semi-analytical solution of the DGLAP evolution as implemented in QCDNUM [6]. Such precision was achieved with $z_m = 1 - 10^{-3}$ and higher z_m gives even better agreement.

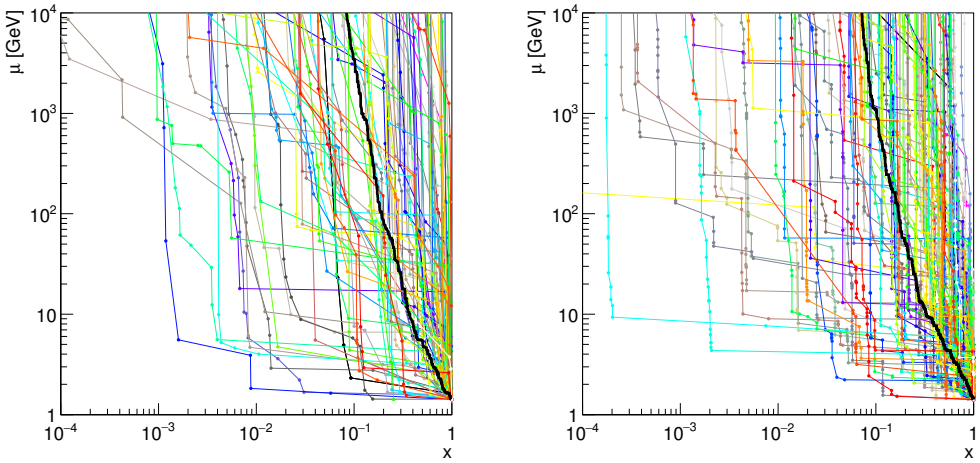

Figure 1: The demonstration of the Parton branching method. For gluon evolving from starting position $\mu = \sqrt{2}$GeV, $x = 1$ towards higher scales. The branchings are represented by dots which are connected by the straight lines. Here, 100 random evolutions have been performed which can be distinguished by different colors. In plot on the left hand side the evolution is shown for $z_m = 1 - 10^{-2}$ whereas on the right hand plot the evolution was performed for $z_m = 1 - 10^{-6}$. The thick black line represents mean trajectory.

3. NNLO evolution

Since the implementation of the NNLO Parton branching evolution is not as straightforward as in LO and NLO case, in this section, we will discuss the aspects which are special for NNLO. As we work with massless quark flavours in variable flavour numbering scheme (VFNS) the number of active flavours appearing in the splitting functions depends on evolutions scale $N_f = N_f(\mu^2)$. Below charm productions threshold which we identify with charm mass m_c there are 3 active flavours, for scales between m_c and m_b there are 4 flavours and so on.

However, only the cross section defined as a convolution of perturbatively calculable coefficient functions and the PDFs is a physical observable and it is naturally assumed to be continuous as a function of scale. Since the coefficient functions also include N_f dependence it was shown [7] that to compensate the discontinuities in coefficient functions at NNLO one needs to introduce discontinuities both in α_s and PDFs (left plot in Fig. 2) on the heavy quark production thresholds. The physical cross section is then continuous function of the scale μ^2.

These PDF discontinuities are given as:

$$\Delta g(x,m_c^2) = \alpha_s^2(m_c^{+2})\,[A_{gq} * q_s + A_{gg} * g] \tag{3.1}$$

$$\Delta q_i(x,m_c^2) = \alpha_s^2(m_c^{+2})\; A_{qq} * q_i \tag{3.2}$$

$$\Delta c(x,m_c^2) = \alpha_s^2(m_c^{+2})\,\left[A_{hq} * q_s + A_{hg} * g\right], \tag{3.3}$$

where m_c^{+2} is infinitely close to m_c^2 from above and e.g. $\Delta g(x,m_c^2) = g(x,m_c^{+2}) - g(x,m_c^{-2})$. The analogous equations with identical convolution kernels A also hold at thresholds corresponding to the bottom mass m_b and top mass m_t. Note that these kernels with their virtual terms satisfy momentum sum rule and, therefore, preserve the unitarity of the DGLAP equation (2.4).

To incorporate these heavy flavours thresholds effects into evolution (2.1), we consider the kernels A as a part of our μ^2-dependent splittings. Formally, we can write:

$$zP_{ab}^{\mathrm{NNLO}}\left(\mu^2,z\right) = zP_{ab}^{\mathrm{reg}}(\mu^2,z) + zA_{ab}(z)\alpha_s^2(m_c^{+2})\,\delta(\log\mu^2 - \log m_c^2) + \{\mathrm{bottom},\mathrm{top}\}, \tag{3.4}$$

where the δ-functions, when integrated over μ^2, result in discontinuities of the Sudakov factor on the heavy quark thresholds (right plot in Fig. 2). Note, that although the both P_{ab}^{reg} and A_{ab} contain virtual terms for $z = 1$ these terms are not used within our MC evolution which conserves unitary by definition.

The procedure for the MC evolution is then the following. We pre-calculate the Sudakov factor for gluon and quark, then in each step of the Markov chain we select the random number r between 0 and 1. The new scale μ_2^2 is chosen in such a way that $\Delta_a(\mu_2^2)/\Delta_a(\mu_1^2) = r$, where μ_1^2 is the original one. In case that the new scale μ_2^2 is on the heavy flavour threshold we select the particular branching type and z-value according to functions A_{ba} instead of standard splitting functions P_{ba}^{reg}. Using such procedure the NNLO Parton branching solution is identical to the semi-analytical DGLAP solution obtained by QCDNUM [6]. We demonstrate this consistency in Fig. 3, the starting PDF parametrisation is given in [2].

4. Effect of intrinsic $\mathbf{k_T}$ and the ordering condition

The main motivation for the Parton branching method is to have PDF dependent not only on x but also on the transverse momentum k_T for all parton flavours. During each branching in the

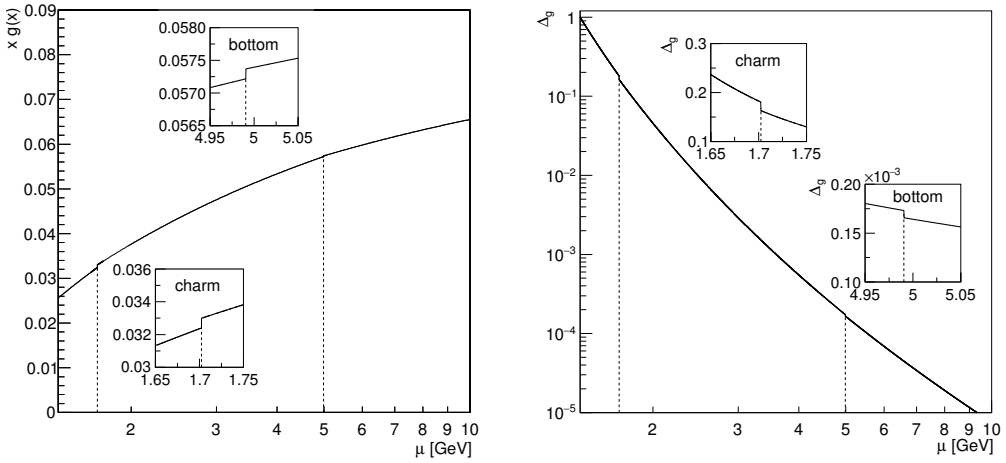

Figure 2: The gluon distribution (left plot) evolved by NNLO DGLAP evolution equations. As the evolution is done in VFNS the discontinuities appear on the heavy quark mass thresholds represented by the dotted lines ($m_c = 1.70\,\text{GeV}$, $m_b = 4.99\,\text{GeV}$). The right plot shows the NNLO Sudakov factor for gluon which is able to handle these discontinuities.

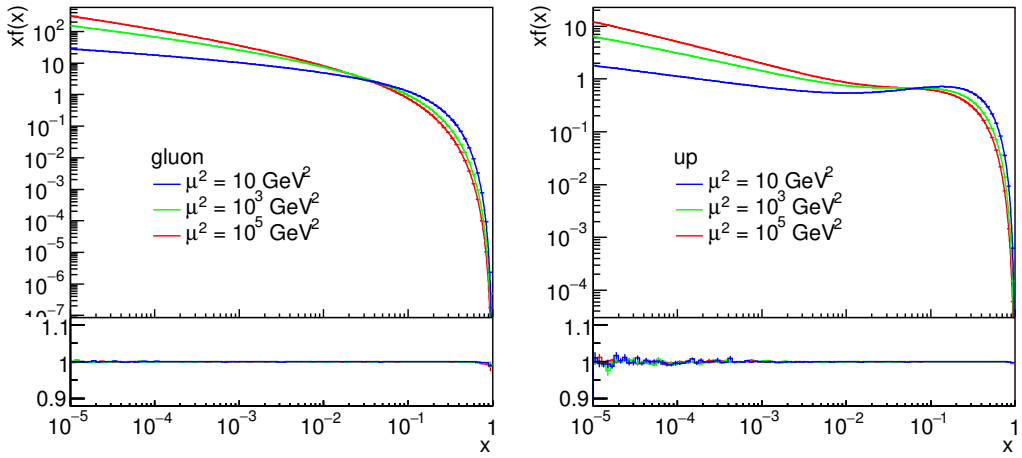

Figure 3: The comparison of the gluon and up-quark PDFs obtained by parton branching method (binned curves) and QCDNUM (smooth curves) at NNLO. The bottom frames show ratio with respect to QCDNUM PDF value.

evolution we generate the transverse momentum q_T of the parton and consequently estimate the final k_T value. The evolution scale μ^2 can be identified either with virtuality or with the angle which corresponds to the formulas:

$$q_T^2 = (1-z)\,Q^2 \overset{\text{def}}{=\!=} (1-z)\;\mu^2, \qquad q_T^2 = (1-z)^2\theta^2 \overset{\text{def}}{=\!=} (1-z)^2\mu^2 \tag{4.1}$$

The angular ordering should include the color coherence effects between the emissions. Both of these definitions are infrared save in such sense that they give $q_T = 0$ when $z \to 1$ and, therefore, the resulting k_T spectrum is well defined in $z_m \to 1$ limit. On the other hand the "naive q_T ordering",

where $q_T^2 \overset{\text{def}}{=\!=} \mu^2$ is not infrared save for $z_m \to 1$ and the infrared emissions must be cut off explicitly by introducing $z_m = z_m(\mu^2) \not\to 1$. However, such type of cut-off affects the collinear evolution as well.

The transverse momentum spectrum of parton densities evolved with angular and virtuality ordering condition (4.1) are compared in Fig. 4. The starting (intrinsic) k_T distribution of transverse momentum dependent densities (TMDs) at scale $\mu_0^2 = 2\,\text{GeV}^2$ was chosen as Gaussian $A(x,k_T,\mu^2) \sim \exp(-k_T^2/2)$ which is assumed to be identical for all flavours. The parametrisation of the collinear part of A at the starting scale can be found in [2]. The normalisation of the TMDs is such that

$$\int_0^\infty \frac{\mathrm{d}^2 k_T}{\pi} A(x,k_T,\mu^2) = \tilde{f}(x,\mu^2). \tag{4.2}$$

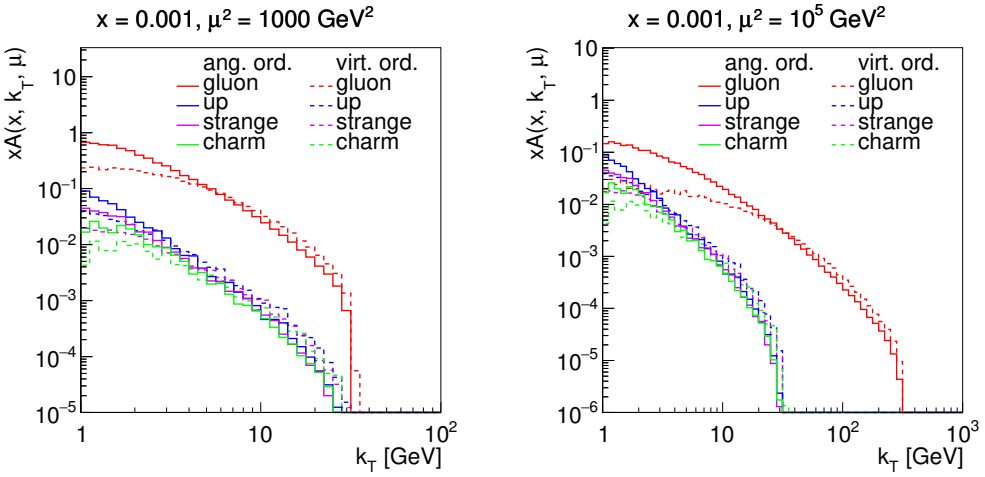

Figure 4: The comparison of transverse momentum spectra for the virtuality and angular ordered evolution.

It can be seen that the ordering conditions differ mostly for high scales μ^2 and low k_T values which is understandable as the starting k_T distributions are identical so when evolved to higher scales more differences are visible. The spectra differ at small k_T since that is the region dominated by soft emissions $z \to 1$ where the difference between the ordering conditions is most prominent.

Furthermore, it can be seen that the quark transverse momentum for virtuality and angular ordering densities differ less than for the gluon one. This is because the quark emits less than gluon, due to different color coefficients in front of the splitting, naively one expects a suppression by $C_A/C_F = 3/\frac{4}{3} = \frac{9}{4}$.

In Fig. 5 we study the effect of the intrinsic momentum of the non-perturbative nature imposed at the beginning of the evolution. We see that the difference in k_T distributions with and without intrinsic k_T at scales $\mu^2 = 10\,\text{GeV}^2$ and $\mu^2 = 1000\,\text{GeV}^2$ is quite small, affecting mainly up-quark at small k_T. It can be easily understood since at μ_0^2 only the gluon and u, d, s quarks are presented. As quarks radiate less the effect of the evolution is smaller and effect of the starting k_T distribution higher.

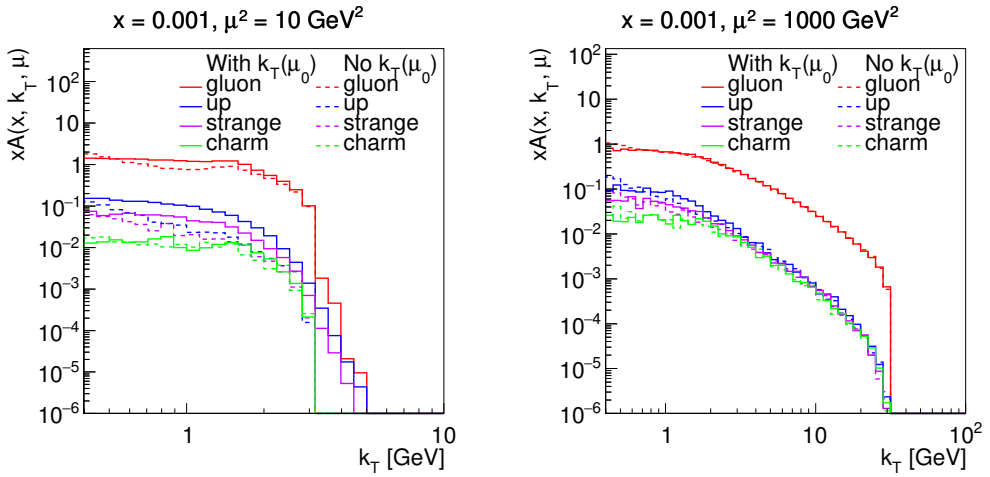

Figure 5: The comparison of the transverse momentum spectra with and without an intrinsic k_T included. Angular ordering condition is used.

5. Conclusion

We have demonstrated some aspects of the Parton branching evolution method and have shown that such formalism can be extended up to NNLO in such a way that the collinear part agrees with the semi-analytical DGLAP solution when the same splitting functions are used and z_m resolution parameter is large enough. We showed that this method allows extracting the k_T spectra for all flavours and that the quark and gluon spectra differ in their average transverse momentum. In addition, we focused on the effect of the ordering condition and intrinsic k_T on the resulting k_T spectrum. The transverse momentum spectrum of parton densities can be tested experimentally for example by the p_T distribution of the Drell-Yann lepton pair or by p_T spectrum of the Higgs boson. The first LO and NLO predictions of the Drell-Yann p_T spectrum obtained using TMDs from the parton branching method were already calculated and will be shown in the future. For the time being our TMDs are based on the corresponding collinear PDFs, dressed by the k_T spectrum during the evolution. The k_T is not considered when calculating the quality of the fit. Nerveless already the current approach allows, for example, to propagate the uncertainties of the collinear PDFs into the k_T spectrum.

References

[1] F. Hautmann, H. Jung, A. Lelek, V. Radescu and R. Zlebcik, *Soft-gluon resolution scale in QCD evolution equations*, *Phys. Lett.* **B772** (2017) 446–451, [1704.01757].

[2] F. Hautmann, H. Jung, A. Lelek, V. Radescu and R. Zlebcik, *Collinear and TMD Quark and Gluon Densities from Parton Branching Solution of QCD Evolution Equations*, 1708.03279.

[3] J. Collins, *Foundations of perturbative QCD*. Cambridge University Press, 2013.

[4] S. Catani, F. Fiorani and G. Marchesini, *Small x Behavior of Initial State Radiation in Perturbative QCD*, *Nucl. Phys.* **B336** (1990) 18–85.

[5] F. Hautmann, M. Hentschinski and H. Jung, *TMD PDFs: A Monte Carlo implementation for the sea quark distribution*, 1205.6358.

[6] M. Botje, *QCDNUM: Fast QCD Evolution and Convolution*, *Comput. Phys. Commun.* **182** (2011) 490–532, [1005.1481].

[7] M. Buza, Y. Matiounine, J. Smith and W. L. van Neerven, *Charm electroproduction viewed in the variable flavor number scheme versus fixed order perturbation theory*, *Eur. Phys. J.* **C1** (1998) 301–320, [hep-ph/9612398].